

Numerical Solution and Analysis of the Vasicek Model for Bond Pricing

Louis Mudarra
CentraleSupélec

February 2025

Abstract

This work is part of the companion project associated with the first-year PDE course at CentraleSupélec. It was originally written in French, and translated using LLM. It addresses the pricing of zero-coupon bonds using the Vasicek model. After reviewing the model's assumptions and presenting the stochastic differential equation, we derive the partial differential equation associated with the model. An analytical solution is obtained and used as a benchmark for the evaluation and comparison of several numerical methods. We detail the implementation in Python of the explicit and implicit Euler schemes, the Crank–Nicolson method, and the finite element method, highlighting the advantages and limitations of each approach. The accuracy of the obtained results confirms the relevance of numerical techniques in quantitative finance. Finally, we demonstrate the robustness and consistency of the model with respect to variations in the target rate and volatility.

Contents

| | | |
|----------|---|-----------|
| 1 | Introduction | 3 |
| 1.1 | Context | 3 |
| 1.2 | Applications | 3 |
| 1.3 | Objectives | 3 |
| 2 | Presentation of the Model | 5 |
| 2.1 | Assumptions | 5 |
| 2.2 | Derivation of the Model's Partial Differential Equation | 5 |
| 3 | Analytical Solution of the PDE | 7 |
| 3.1 | Characterization of the PDE | 7 |
| 3.2 | Exact Solution | 7 |
| 4 | Explicit Euler Method | 9 |
| 4.1 | Change of Variables and Discretization | 9 |
| 4.2 | Spatial Approximation | 10 |
| 4.3 | Explicit Temporal Approximation | 10 |
| 4.4 | Implementation in Python | 10 |
| 5 | Implicit Euler Method | 14 |
| 5.1 | Spatial Approximation | 14 |
| 5.2 | Implicit Temporal Approximation | 14 |
| 5.3 | Definition of the Tridiagonal System | 15 |
| 5.4 | Implementation in Python | 15 |
| 6 | Crank–Nicolson Method | 20 |
| 6.1 | Definition of the Scheme and Derivation of the System | 20 |
| 6.2 | Implementation in Python | 21 |
| 7 | Finite Element Method | 24 |
| 7.1 | Definition of the Sobolev Spaces | 24 |
| 7.2 | Variational Formulation | 25 |
| 7.3 | Discretization with \mathbb{P}_1 Finite Elements | 26 |
| 7.4 | Analysis of the ODE System | 27 |
| 7.5 | Implementation in Python | 27 |
| 8 | Sensitivity Analysis with Respect to Parameters | 30 |
| 8.1 | Sensitivity with Respect to the Target Rate γ | 30 |
| 8.2 | Sensitivity with Respect to the Volatility σ | 31 |
| 9 | Conclusion | 33 |

1 Introduction

1.1 Context

The Vasicek model is employed to describe the evolution of short-term interest rates. It was first introduced by Oldřich Vasicek in 1977 in his article “An equilibrium characterization of the term structure” [1].

Although the application of stochastic calculus in finance—especially for pricing financial instruments—was already well established before Vasicek (Samuelson 1973 [2], Black–Scholes 1973 [3], Merton 1974 [4], etc.), his approach remains innovative in modeling the behavior of interest rates via a mean-reversion mechanism.

By considering the instantaneous interest rate as following an Ornstein–Uhlenbeck process, Vasicek laid the groundwork for a new class of models that have become indispensable in quantitative finance and financial mathematics (e.g., CIR [5], Hull–White [6], etc.).

1.2 Applications

The Vasicek model is primarily used to price simple financial instruments that depend directly on time and the interest rate, such as zero-coupon bonds. It also serves as a foundation for modeling more complex products, such as swaps or caps and floors, although their valuation may require additional assumptions on volatility or cash flow structures.

Moreover, the model is a useful tool in risk management, particularly for assessing interest rate risk exposure and simulating stress scenarios for bond portfolios. It can also be integrated into the calculation of capital requirements in accordance with international standards such as Basel III (2010).

1.3 Objectives

The objective is to price zero-coupon bonds by studying the PDE associated with the Vasicek model. In Section 2, we present the Vasicek model by recalling its fundamental assumptions, and then derive the partial differ-

ential equation governing the bond price using Itô’s lemma along with the stochastic differential equation describing the evolution of the interest rate. In Section 3, an analytical solution of this equation is obtained, which will serve as a reference for the numerical analysis. In Section 4, we detail the application of the explicit Euler scheme. Section 5 is devoted to the implementation of the implicit Euler scheme, where the resulting tridiagonal system is solved using the Thomas algorithm. In Section 6, the Crank–Nicolson method is presented, also employing the Thomas algorithm and offering the best performance in terms of accuracy. Finally, in Section 7, we detail the application of the finite element method. Once the numerical approaches have been examined, we focus our study on the sensitivity of bond prices to the model parameters. In particular, in Section 8 we examine in detail the influence of the target rate and volatility.

2 Presentation of the Model

2.1 Assumptions

The fundamental assumptions formulated by Vasicek are as follows:

- The instantaneous interest rate r_t is a continuous function of time that follows a Markov process.
- The price of a zero-coupon bond depends solely on time and the instantaneous interest rate. In particular, this rate is the only state variable in the model. We therefore assume that r_t contains all the information necessary to determine bond prices and, by extension, to construct the yield curve.
- There is no arbitrage opportunity. Any potential profit is the result of previously assumed risk, which is correctly reflected in the price. This assumption ensures market price consistency and permits the use of a risk-neutral measure for asset valuation.
- The market price of risk is constant. Taking on additional risk is compensated proportionally to the amount of risk assumed.

2.2 Derivation of the Model's Partial Differential Equation

The instantaneous interest rate r_t follows the stochastic differential equation (SDE):

$$dr_t = \kappa(\gamma - r_t) dt + \sigma dW_t \quad (1)$$

where:

- W_t is a standard Brownian motion.
- r_t is the primary variable representing the short-term interest rate.
- σ represents the volatility of the interest rate.
- γ is the long-term mean (target rate) towards which r_t reverts.
- κ is the speed of mean reversion of r_t towards γ .

From this SDE, we derive the following partial differential equation (PDE) that describes the price $V(r, t)$ of a zero-coupon bond maturing at time T :

$$\frac{1}{2}\sigma^2 \frac{\partial^2 V}{\partial r^2} + \kappa(\gamma - r) \frac{\partial V}{\partial r} + \frac{\partial V}{\partial t} - rV = 0. \quad (2)$$

Proof:

Consider $V(r, t)$, the price of a zero-coupon bond at time t when the instantaneous rate is r , with maturity T . By applying Itô's lemma to $V(r, t)$, we have:

$$dV = \frac{\partial V}{\partial t} dt + \frac{\partial V}{\partial r} dr + \frac{1}{2} \frac{\partial^2 V}{\partial r^2} (dr)^2. \quad (3)$$

Substituting $dr = \kappa(\gamma - r) dt + \sigma dW_t$ and noting that $(dW_t)^2 = dt$, we obtain:

$$dV = \frac{\partial V}{\partial t} dt + \frac{\partial V}{\partial r} [\kappa(\gamma - r) dt + \sigma dW_t] + \frac{1}{2} \frac{\partial^2 V}{\partial r^2} \sigma^2 dt. \quad (4)$$

That is,

$$dV = \left[\frac{\partial V}{\partial t} + \kappa(\gamma - r) \frac{\partial V}{\partial r} + \frac{1}{2} \sigma^2 \frac{\partial^2 V}{\partial r^2} \right] dt + \sigma \frac{\partial V}{\partial r} dW_t. \quad (5)$$

Under the risk-neutral measure \mathbb{Q} and in the absence of arbitrage, we have:

$$\mathbb{E}^{\mathbb{Q}}[dV] = rV dt \quad \text{and} \quad \mathbb{E}^{\mathbb{Q}}[dW_t] = 0. \quad (6)$$

By linearity of the expectation operator and considering only the deterministic terms, it follows that:

$$rV dt = \left(\frac{\partial V}{\partial t} + \kappa(\gamma - r) \frac{\partial V}{\partial r} + \frac{1}{2} \sigma^2 \frac{\partial^2 V}{\partial r^2} \right) dt. \quad (7)$$

Equivalently,

$$\frac{\partial V}{\partial t} + \kappa(\gamma - r) \frac{\partial V}{\partial r} + \frac{1}{2} \sigma^2 \frac{\partial^2 V}{\partial r^2} - rV = 0. \quad (8)$$

By the properties of a bond, we have the following terminal condition: at maturity ($t = T$), the bond is worth its face value. Hence,

$$V(r, T) = 1. \quad (9)$$

3 Analytical Solution of the PDE

In this section, we present the explicit solution of the PDE derived from the Vasicek model. Indeed, unlike more complex models, the PDE associated with the Vasicek model admits a closed-form solution. The goal of this section is to provide a detailed derivation of this solution, which will later serve as a reference for numerical comparisons.

3.1 Characterization of the PDE

The PDE associated with the Vasicek model is given by:

$$\frac{\partial V}{\partial t} + \kappa(\gamma - r)\frac{\partial V}{\partial r} + \frac{1}{2}\sigma^2\frac{\partial^2 V}{\partial r^2} - rV = 0. \quad (10)$$

A general linear second-order PDE in the variables (r, t) can be written as:

$$A\frac{\partial^2 V}{\partial r^2} + B\frac{\partial^2 V}{\partial r \partial t} + C\frac{\partial^2 V}{\partial t^2} + D\frac{\partial V}{\partial r} + E\frac{\partial V}{\partial t} + FV = 0, \quad (11)$$

with the discriminant given by:

$$\Delta = B^2 - 4AC. \quad (12)$$

Considering the values of the coefficients A , B , and C , we immediately obtain $\Delta = 0$. Hence, the PDE is parabolic.

Knowing that the PDE is parabolic gives us insight into the form of its solution.

3.2 Exact Solution

We seek a solution of the form

$$V(r, t) = A(t, T)e^{-B(t, T)r}. \quad (13)$$

We then compute the derivatives:

$$\frac{\partial V}{\partial t} = \left(\frac{\partial A}{\partial t} - A \frac{\partial B}{\partial t} r \right) e^{-B r}, \quad (14)$$

$$\frac{\partial V}{\partial r} = -B A e^{-Br}, \quad (15)$$

$$\frac{\partial^2 V}{\partial r^2} = B^2 A e^{-Br}. \quad (16)$$

Substituting these derivatives into the Vasicek PDE, we obtain:

$$\left(\frac{\partial A}{\partial t} - A \frac{\partial B}{\partial t} r \right) e^{-Br} - \kappa(\gamma - r) B A e^{-Br} + \frac{1}{2} \sigma^2 B^2 A e^{-Br} - r A e^{-Br} = 0. \quad (17)$$

This leads to the following equations for $B(t, T)$ and $A(t, T)$:

$$-\frac{\partial B}{\partial t} + \kappa B - 1 = 0, \quad (18)$$

$$\frac{\partial A}{\partial t} + A \left(\frac{1}{2} \sigma^2 B^2 - \kappa \gamma B \right) = 0. \quad (19)$$

With the terminal conditions $B(T, T) = 0$ and $A(T, T) = 1$, we obtain:

$$B(t, T) = \frac{1 - e^{-\kappa(T-t)}}{\kappa}, \quad (20)$$

$$A(t, T) = \exp \left\{ \left(\gamma - \frac{\sigma^2}{2\kappa^2} \right) (B(t, T) - (T-t)) - \frac{\sigma^2}{4\kappa} B^2(t, T) \right\}. \quad (21)$$

Thus, with $A(t, T)$ and $B(t, T)$ defined as above, we have

$$V(r, t) = A(t, T) e^{-B(t,T)r}. \quad (22)$$

4 Explicit Euler Method

The first numerical method employed is the simplest, as it provides a straightforward recurrence relation that can be easily implemented in Python. The objective is to clearly define the numerical method and study its performance via simulation. Subsequently, other, sometimes more sophisticated methods will be analyzed using the same approach.

4.1 Change of Variables and Discretization

To apply numerical methods, it is necessary to introduce meshes to discretize the domains of the variables. For convenience, we also perform the time transformation:

$$\tau = T - t, \quad (23)$$

and define the transformed function:

$$Q(\tau, r) = V(r, T - \tau), \quad (24)$$

so that the terminal condition becomes an initial condition:

$$Q(0, r) = 1. \quad (25)$$

We also define the set of possible interest rates as:

$$\Omega = [0, r_{\max}], \quad (26)$$

where r_{\max} is the maximum expected interest rate (fixed but context-dependent). The spatial mesh of Ω is defined as:

$$r_i = i \Delta r \quad \text{for } i = 0, 1, \dots, M, \quad \text{with } \Delta r = \frac{r_{\max}}{M}. \quad (27)$$

The time mesh in τ , spanning the life of the bond $[0, T]$ (with T the maturity), is defined as:

$$\tau^n = n \Delta \tau \quad \text{for } n = 0, 1, \dots, N, \quad \text{with } \Delta \tau = \frac{T}{N}. \quad (28)$$

The numerical solution is thus evaluated at the mesh points and denoted:

$$Q_i^n = Q(\tau^n, r_i). \quad (29)$$

4.2 Spatial Approximation

The spatial derivatives with respect to r at the mesh points are approximated using centered differences:

$$\frac{\partial Q}{\partial r} \Big|_{r=r_i} \approx \frac{Q_{i+1}^n - Q_{i-1}^n}{2 \Delta r}, \quad (30)$$

$$\frac{\partial^2 Q}{\partial r^2} \Big|_{r=r_i} \approx \frac{Q_{i+1}^n - 2Q_i^n + Q_{i-1}^n}{(\Delta r)^2}. \quad (31)$$

4.3 Explicit Temporal Approximation

In the explicit Euler scheme, the time derivative at the mesh point (τ^n, r_i) is approximated using a forward difference:

$$\frac{\partial Q}{\partial \tau} \Big|_{\tau=\tau^n} \approx \frac{Q_i^{n+1} - Q_i^n}{\Delta \tau}. \quad (32)$$

Thus, the explicit Euler scheme is defined by the recurrence relation:

$$Q_i^{n+1} = Q_i^n + \Delta \tau L_i^n, \quad (33)$$

for $i = 1, \dots, M-1$, where L_i^n is given by:

$$L_i^n = \kappa(\gamma - r_i) \frac{Q_{i+1}^n - Q_{i-1}^n}{2 \Delta r} + \frac{1}{2} \sigma^2 \frac{Q_{i+1}^n - 2Q_i^n + Q_{i-1}^n}{(\Delta r)^2} - r_i Q_i^n. \quad (34)$$

4.4 Implementation in Python

This scheme is easier to implement than the following methods. The implementation involves iterating over the time steps and, for each point in the interior of Ω (i.e., for all $i = 1, \dots, M-1$), computing Q_i^n using the recurrence relation:

$$Q_i^{n+1} = Q_i^n + \Delta \tau L_i^n. \quad (35)$$

Boundary conditions are imposed using the analytical solution.

We use **matplotlib** to plot in 3D the numerical approximations obtained as functions of (r, t) , and compare them with the analytical solution.

For the simulations, we use the following parameters, chosen arbitrarily but consistent with the context of zero-coupon bonds:

$$\kappa = 0.1, \quad \gamma = 0.05, \quad \sigma = 0.01, \quad T = 1.0, \quad r_{\max} = 0.15, \quad N = 100, \quad M = 50.$$

Figure 1 displays a surface that is coherent with the chosen parameters and seems to adequately reflect the price of a zero-coupon bond as a function of r and t . It is then necessary to plot the surface corresponding to the analytical solution (Figure 2) to assess the quality of the numerical approach relative to the analytical solution.

Recall that the analytical solution is given in Section 3 in the form: $A(t, T)e^{-B(t, T)r}$.

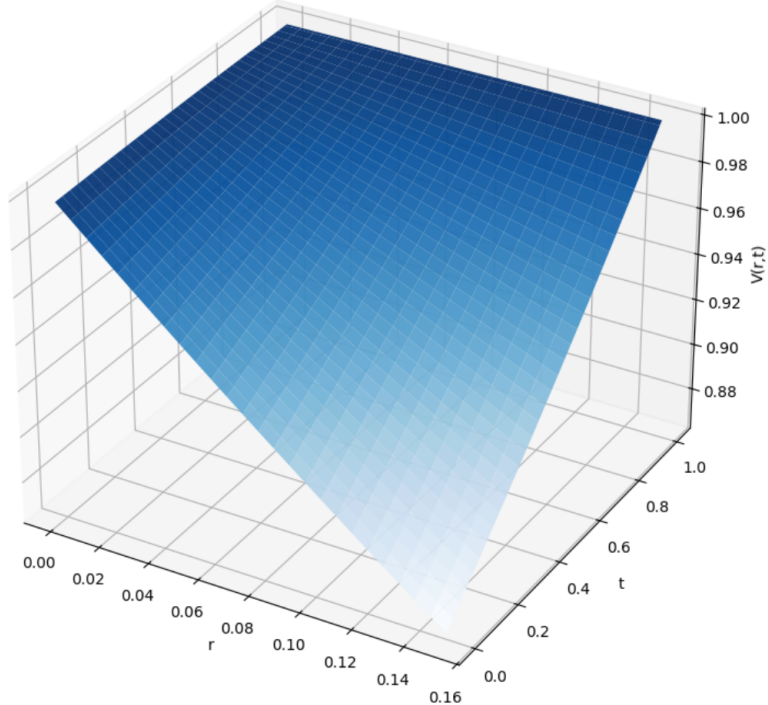


Figure 1: Approximation of the Vasicek model PDE solution using the explicit Euler method

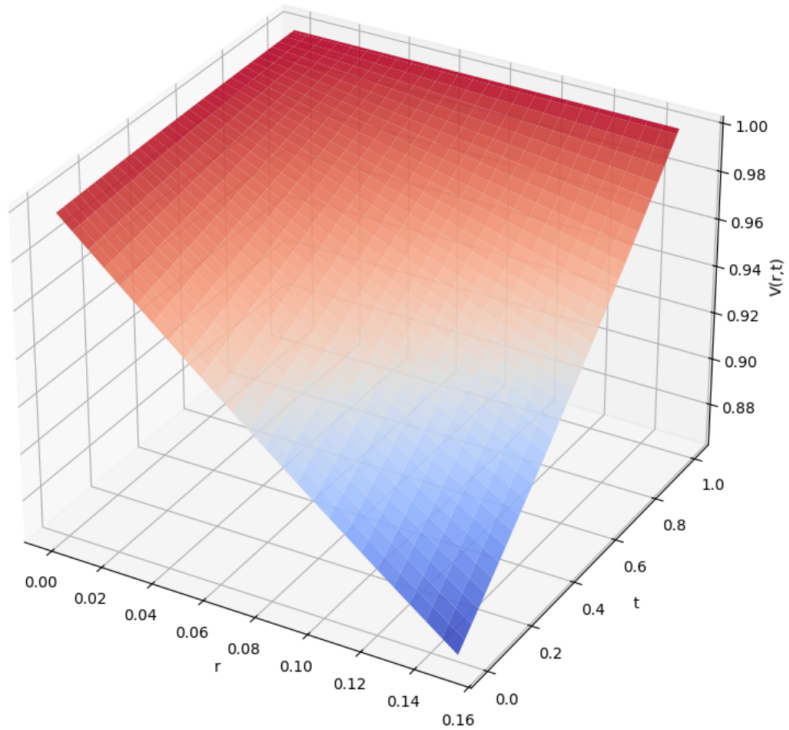


Figure 2: Analytical solution of the Vasicek model PDE

At first glance, the two results are very similar. To verify this, we plot the surface corresponding to the error of the numerical approach, defined simply as:

$$e(r, t) = |V_{\text{numerical}}(r, t) - V_{\text{analytical}}(r, t)| . \quad (36)$$

Figure 3 confirms our initial observation, with the error being on the order of 10^{-5} . Thus, the explicit Euler method is effective in approximating the solution of the Vasicek model PDE.

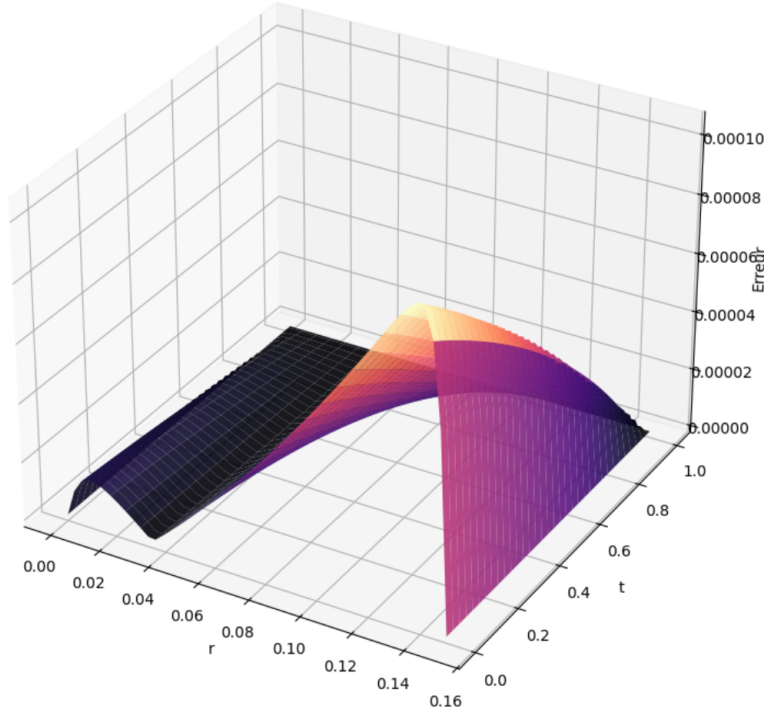


Figure 3: Error of the explicit Euler approximation relative to the analytical solution

5 Implicit Euler Method

In this section, we apply the implicit Euler method to obtain a numerical approximation of the PDE solution. Although this method remains relatively simple, it is more involved than the explicit Euler method (discussed in Section 4) due to the temporal derivative approximation, which does not yield a direct recurrence relation. However, the structure of the resulting system allows the use of the Thomas algorithm for efficient resolution. The goal of this section is to evaluate the numerical approximation relative both to the analytical solution and to the explicit Euler method.

We use the same change of variables and discretization as in the explicit Euler approach:

$$\tau = T - t, \quad Q(\tau, r) = V(r, T - \tau), \quad Q_i^n = Q(\tau^n, r_i). \quad (37)$$

5.1 Spatial Approximation

The spatial derivatives at time level $n + 1$ are approximated at the mesh points using centered differences:

$$\frac{\partial Q}{\partial r} \Big|_{r=r_i}^{n+1} \approx \frac{Q_{i+1}^{n+1} - Q_{i-1}^{n+1}}{2 \Delta r}, \quad (38)$$

$$\frac{\partial^2 Q}{\partial r^2} \Big|_{r=r_i}^{n+1} \approx \frac{Q_{i+1}^{n+1} - 2Q_i^{n+1} + Q_{i-1}^{n+1}}{(\Delta r)^2}. \quad (39)$$

5.2 Implicit Temporal Approximation

In the implicit Euler scheme, the time derivative is approximated at (τ^{n+1}, r_i) using a backward difference:

$$\frac{\partial Q}{\partial \tau} \Big|_{\tau=\tau^{n+1}} \approx \frac{Q_i^{n+1} - Q_i^n}{\Delta \tau}. \quad (40)$$

Thus, the implicit scheme is written as:

$$Q_i^{n+1} - \Delta \tau L_i^{n+1} = Q_i^n, \quad (41)$$

for $i = 1, \dots, M - 1$, where

$$L_i^{n+1} = \kappa(\gamma - r_i) \frac{Q_{i+1}^{n+1} - Q_{i-1}^{n+1}}{2\Delta r} + \frac{1}{2}\sigma^2 \frac{Q_{i+1}^{n+1} - 2Q_i^{n+1} + Q_{i-1}^{n+1}}{(\Delta r)^2} - r_i Q_i^{n+1}. \quad (42)$$

This yields the following equation relating Q_i^n , Q_{i-1}^{n+1} , Q_i^{n+1} , and Q_{i+1}^{n+1} :

$$\begin{aligned} Q_i^n = & -\Delta\tau \left(\frac{\sigma^2}{2(\Delta r)^2} - \frac{\kappa(\gamma - r_i)}{2\Delta r} \right) Q_{i-1}^{n+1} \\ & + \left(1 + \Delta\tau \left(r_i + \frac{\sigma^2}{(\Delta r)^2} \right) \right) Q_i^{n+1} \\ & - \Delta\tau \left(\frac{\sigma^2}{2(\Delta r)^2} + \frac{\kappa(\gamma - r_i)}{2\Delta r} \right) Q_{i+1}^{n+1}. \end{aligned} \quad (43)$$

5.3 Definition of the Tridiagonal System

The set of equations for $i = 1, \dots, M - 1$ forms a tridiagonal linear system that can be written as:

$$-\alpha_i Q_{i-1}^{n+1} + \beta_i Q_i^{n+1} - \gamma_i Q_{i+1}^{n+1} = Q_i^n, \quad (44)$$

where the coefficients α_i , β_i , and γ_i are defined as:

$$\alpha_i = \Delta\tau \left(\frac{1}{2} \frac{\sigma^2}{(\Delta r)^2} - \frac{\kappa(\gamma - r_i)}{2\Delta r} \right), \quad (45)$$

$$\beta_i = 1 + \Delta\tau \left(r_i + \frac{\sigma^2}{(\Delta r)^2} \right), \quad (46)$$

$$\gamma_i = \Delta\tau \left(\frac{1}{2} \frac{\sigma^2}{(\Delta r)^2} + \frac{\kappa(\gamma - r_i)}{2\Delta r} \right). \quad (47)$$

Boundary conditions at r_0 and r_M are imposed via the analytical solution. To incorporate these conditions into the system, the right-hand side is adjusted as follows:

$$d_1 = Q_1^n + \alpha_1 Q_0^{n+1}, \quad d_{M-1} = Q_{M-1}^n + \gamma_{M-1} Q_M^{n+1}. \quad (48)$$

5.4 Implementation in Python

For the Python implementation of the implicit Euler approach, the tridiagonal linear system (Equation (43)) is solved at each time step using the Thomas algorithm [7].

The same numerical parameter values as before are used:

$$\kappa = 0.1, \quad \gamma = 0.05, \quad \sigma = 0.01, \quad T = 1.0, \quad r_{\max} = 0.15, \quad N = 100, \quad M = 50.$$

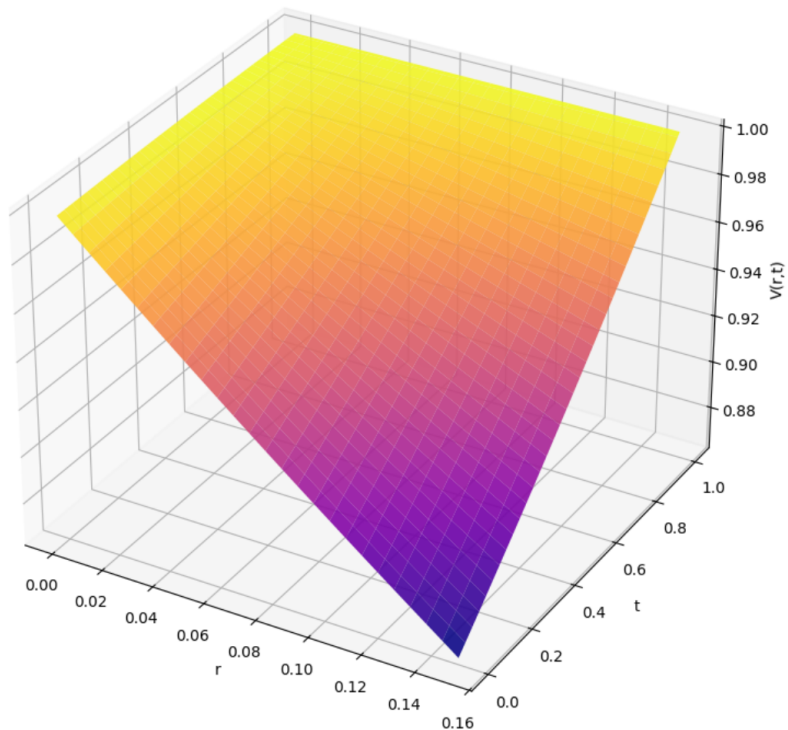


Figure 4: Approximation of the Vasicek model PDE solution using the implicit Euler method

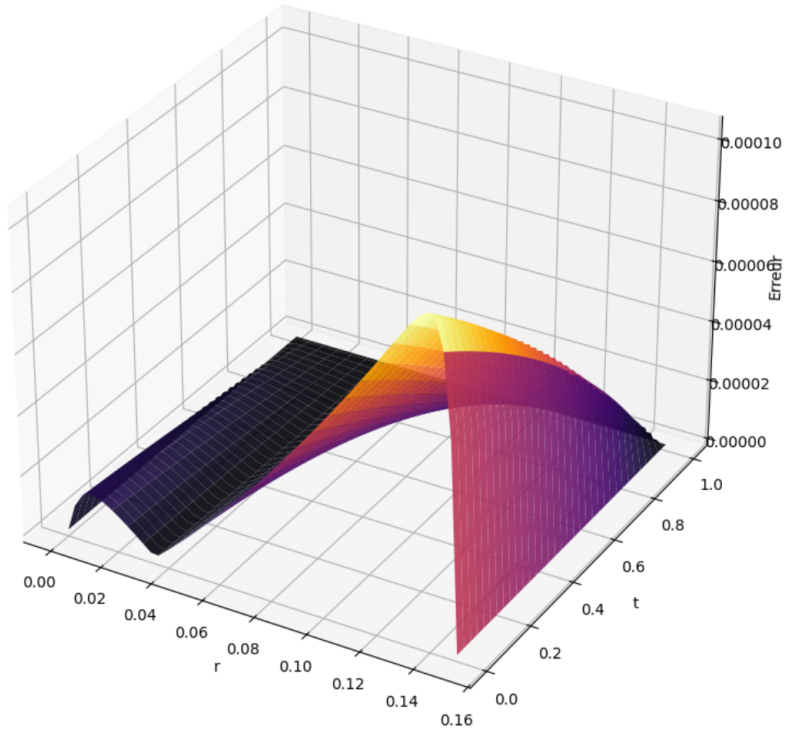


Figure 5: Error of the implicit Euler approximation relative to the analytical solution

Figure 4 shows the numerical approximation obtained. As with the explicit Euler method, it agrees well with the analytical solution (see Figure 2). This is confirmed by Figure 5, which depicts the error $e(r, t)$ between the analytical solution and the numerical approximation defined in (35).

As in the explicit Euler simulation, the error is of the order of 10^{-5} . The implicit Euler method, implemented using the Thomas algorithm, is thus effective in this context.

It is also instructive to compare the approximations obtained with the explicit and implicit Euler methods. By plotting, as a function of (r, t) , the difference defined by:

$$V_{\text{explicite}}(r, t) - V_{\text{implicite}}(r, t), \quad (49)$$

we obtain Figure 6, which shows that $V_{\text{explicite}} \leq V_{\text{implicite}}$. In particular, at its minimum, the difference is approximately 2×10^{-4} . Considering the minimal errors of both methods relative to the analytical solution, one can write in the neighborhood of the minimizer of $(r, t) \mapsto V_{\text{explicite}}(r, t) - V_{\text{implicite}}(r, t)$:

$$V_{\text{explicite}}(r, t) \leq V(r, t) \leq V_{\text{implicite}}(r, t). \quad (50)$$

Such a result was expected and is consistent with the nature of the two schemes.

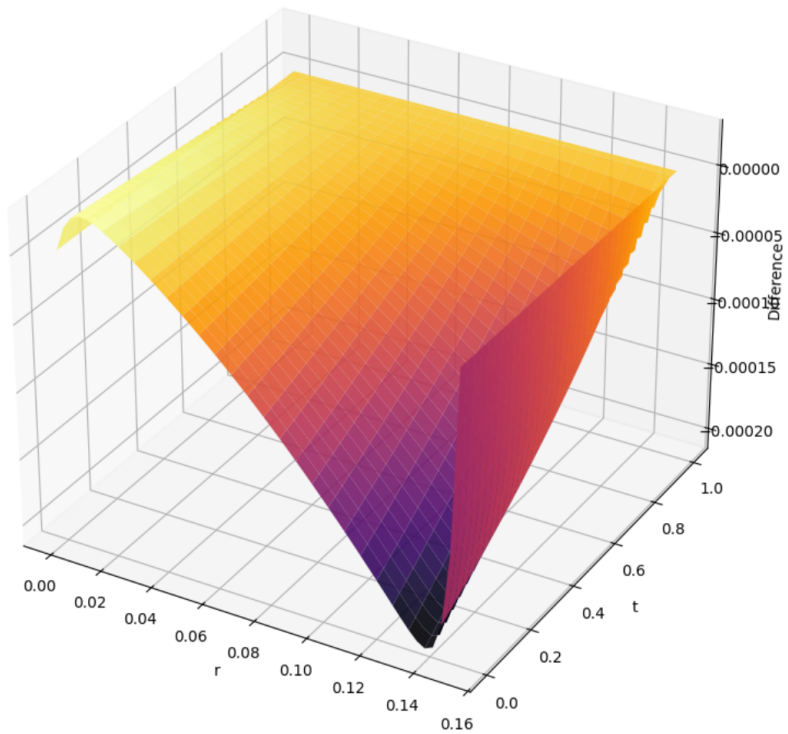


Figure 6: Difference between the implicit Euler and explicit Euler approximations

6 Crank–Nicolson Method

In this section, we apply the Crank–Nicolson finite difference method to obtain a numerical approximation of the solution of the Vasicek PDE. The approach is similar to that in the previous sections; hence, detailed derivations are omitted and the final relation linking the values of Q at the mesh points is given directly. The goal is to assess whether a priori more sophisticated methods yield results that more accurately match the analytical solution.

We use the same change of variables and discretization as in Sections 4 and 5:

$$\tau = T - t, \quad Q(\tau, r) = V(r, T - \tau), \quad Q_i^n = Q(\tau^n, r_i). \quad (51)$$

6.1 Definition of the Scheme and Derivation of the System

The Crank–Nicolson scheme approximates the time derivative using a centered difference and takes the average of the spatial operators at times τ^n and τ^{n+1} . For each interior mesh point $i = 1, \dots, M - 1$, the full equation, with all approximations, reads:

$$\begin{aligned} \frac{Q_i^{n+1} - Q_i^n}{\Delta\tau} &= \frac{1}{2} \left[\kappa(\gamma - r_i) \frac{Q_{i+1}^{n+1} - Q_{i-1}^{n+1}}{2\Delta r} \right. \\ &\quad + \frac{1}{2}\sigma^2 \frac{Q_{i+1}^{n+1} - 2Q_i^{n+1} + Q_{i-1}^{n+1}}{(\Delta r)^2} - r_i Q_i^{n+1} \\ &\quad \left. + \kappa(\gamma - r_i) \frac{Q_{i+1}^n - Q_{i-1}^n}{2\Delta r} + \frac{1}{2}\sigma^2 \frac{Q_{i+1}^n - 2Q_i^n + Q_{i-1}^n}{(\Delta r)^2} - r_i Q_i^n \right]. \end{aligned} \quad (52)$$

As in the implicit Euler study, the equation can be rearranged into a tridiagonal linear system of the form:

$$-\lambda_i Q_{i-1}^{n+1} + (1 + \theta_i) Q_i^{n+1} - \mu_i Q_{i+1}^{n+1} = \lambda_i Q_{i-1}^n + (1 - \theta_i) Q_i^n + \mu_i Q_{i+1}^n, \quad (53)$$

where the coefficients λ_i , μ_i , and θ_i are defined by:

$$\lambda_i = \frac{\Delta\tau}{4\Delta r} \kappa(\gamma - r_i) + \frac{\Delta\tau}{4} \frac{\sigma^2}{(\Delta r)^2}, \quad (54)$$

$$\mu_i = -\frac{\Delta\tau}{4\Delta r} \kappa(\gamma - r_i) + \frac{\Delta\tau}{4} \frac{\sigma^2}{(\Delta r)^2}, \quad (55)$$

$$\theta_i = \frac{\Delta\tau}{2} \left(\frac{\sigma^2}{(\Delta r)^2} + r_i \right). \quad (56)$$

6.2 Implementation in Python

For the implementation of this scheme, we again use the Thomas algorithm to solve the resulting tridiagonal system. The same parameters as in previous simulations are used:

$$\kappa = 0.1, \quad \gamma = 0.05, \quad \sigma = 0.01, \quad T = 1.0, \quad r_{\max} = 0.15, \quad N = 100, \quad M = 50.$$

This yields the 3D plot of the numerical approximation of the bond price as a function of (r, t) (see Figure 7), as well as the error relative to the analytical solution (Figure 8).

The error is now on the order of 10^{-8} , representing a significant improvement over the Euler schemes. Thus, the Crank–Nicolson scheme is particularly effective in this context, despite being more complex to implement than the explicit Euler method.

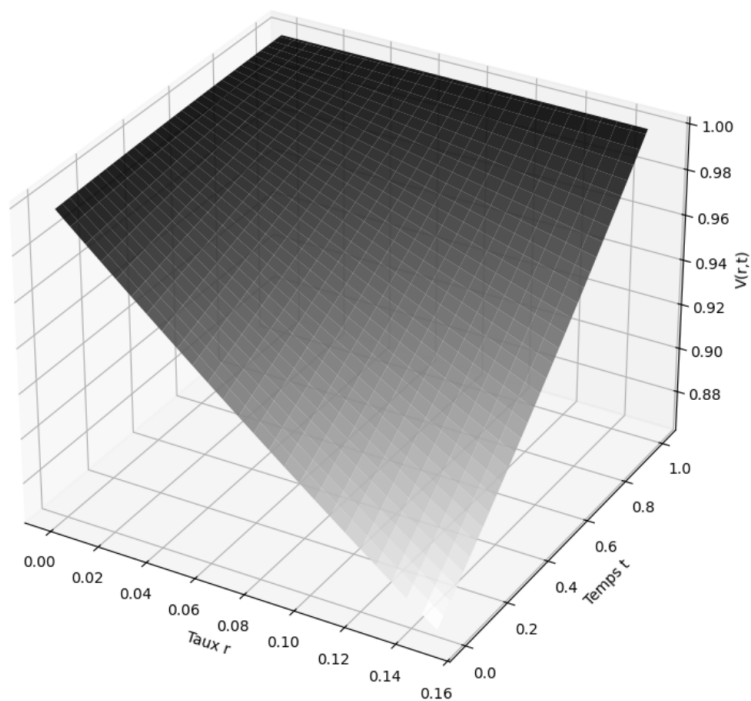


Figure 7: Approximation of the Vasicek model PDE solution using the Crank–Nicolson method

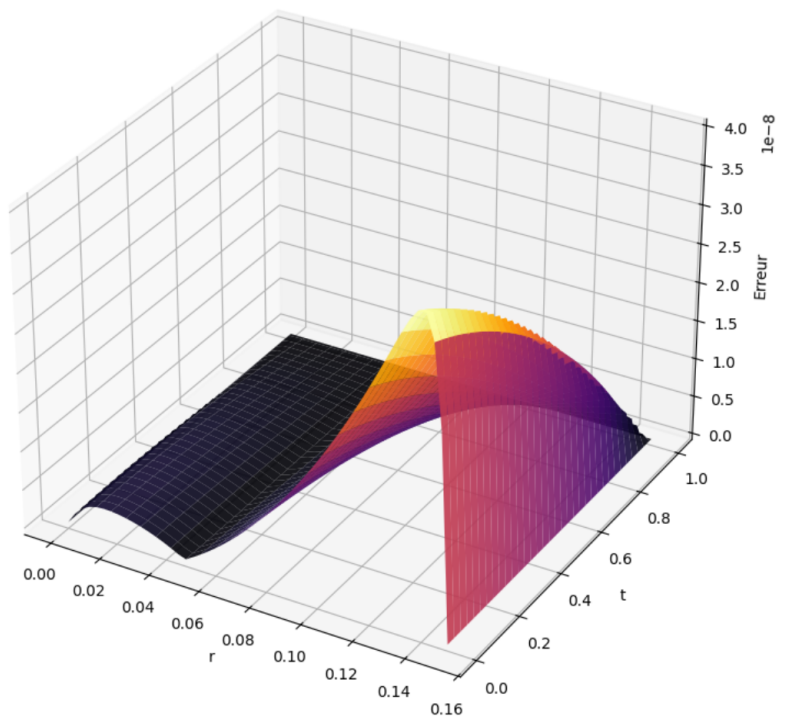


Figure 8: Error of the Crank–Nicolson approximation relative to the analytical solution

7 Finite Element Method

In this section, we apply the finite element method (FEM) to numerically approximate the solution of the Vasicek model PDE. We begin by defining the appropriate Sobolev spaces, derive the variational formulation of the problem, and then discretize using \mathbb{P}_1 finite elements. Finally, we present the graphical approximation obtained by applying the Crank–Nicolson method to the resulting matrix ODE, and compare the results with the analytical solution.

We again use the change of variable:

$$Q(\tau, r) = V(r, T - t).$$

7.1 Definition of the Sobolev Spaces

Let $\Omega \subset \mathbb{R}^d$ be an open set. The Sobolev space $H^1(\Omega)$ is defined by:

$$H^1(\Omega) = \{u \in L^2(\Omega) \mid \nabla u \in L^2(\Omega)\}, \quad (57)$$

where ∇u denotes the distributional gradient of u .

We then define the space $H_0^1(\Omega)$ as:

$$H_0^1(\Omega) = \{u \in H^1(\Omega) \mid u|_{\partial\Omega} = 0\}. \quad (58)$$

In the particular case $\Omega = (0, r_{\max})$, we have:

$$H^1(\Omega) = \{u \in L^2(0, r_{\max}) \mid u' \in L^2(0, r_{\max})\}. \quad (59)$$

Finally, the space $H_0^1(\Omega)$ is defined as:

$$H_0^1(\Omega) = \{u \in H^1(\Omega) \mid u(0) = u(r_{\max}) = 0\}. \quad (60)$$

Having defined the necessary spaces, we now derive the variational formulation of our PDE. Consider a test function $\omega \in H_0^1(\Omega)$, where $\Omega = (0, r_{\max})$.

7.2 Variational Formulation

Starting from the PDE:

$$-\frac{\partial Q}{\partial \tau} + \kappa(\gamma - r) \frac{\partial Q}{\partial r} + \frac{1}{2} \sigma^2 \frac{\partial^2 Q}{\partial r^2} - rQ = 0, \quad (61)$$

we multiply by a test function $\omega \in H_0^1(\Omega)$ and integrate over Ω :

$$\int_{\Omega} \left(-\frac{\partial Q}{\partial \tau} + \kappa(\gamma - r) \frac{\partial Q}{\partial r} + \frac{1}{2} \sigma^2 \frac{\partial^2 Q}{\partial r^2} - rQ \right) \omega \, dr = 0. \quad (62)$$

Applying Green's formula to the second derivative term yields:

$$\int_{\Omega} \left(-\frac{\partial Q}{\partial \tau} \omega + \kappa(\gamma - r) \frac{\partial Q}{\partial r} \omega - \frac{1}{2} \sigma^2 \frac{\partial Q}{\partial r} \frac{\partial \omega}{\partial r} - rQ \omega \right) \, dr = 0. \quad (63)$$

By differentiating under the integral sign, we have:

$$\int_{\Omega} \frac{\partial Q}{\partial \tau} \omega \, dr = \frac{d}{d\tau} \int_{\Omega} Q \omega \, dr. \quad (64)$$

Thus,

$$-\frac{d}{d\tau} \int_{\Omega} Q \omega \, dr + \int_{\Omega} \left[\kappa(\gamma - r) \frac{\partial Q}{\partial r} \omega - \frac{1}{2} \sigma^2 \frac{\partial Q}{\partial r} \frac{\partial \omega}{\partial r} - rQ \omega \right] \, dr = 0, \quad (65)$$

for all $\omega \in H_0^1(\Omega)$.

We then define the bilinear forms a and b as:

$$a(Q, \omega) = \int_{\Omega} Q \omega \, dr, \quad (66)$$

$$b(Q, \omega) = \int_{\Omega} \left[\kappa(\gamma - r) \frac{\partial Q}{\partial r} \omega - \frac{1}{2} \sigma^2 \frac{\partial Q}{\partial r} \frac{\partial \omega}{\partial r} - rQ \omega \right] \, dr. \quad (67)$$

The weak formulation of the problem is therefore:

$$\forall \omega \in H_0^1(\Omega), \quad -\frac{d}{d\tau} a(Q, \omega) + b(Q, \omega) = 0. \quad (68)$$

7.3 Discretization with \mathbb{P}_1 Finite Elements

To approximate the solution Q , we use the same spatial discretization of Ω as before:

$$r_i = i \Delta r \quad \text{for } i = 0, 1, \dots, M, \quad \text{with } \Delta r = \frac{r_{\max}}{M}. \quad (69)$$

We consider the finite element space $S_h \subset H_0^1(\Omega)$, consisting of functions that are piecewise affine over each interval of the mesh:

$$S_h = \{v \in H_0^1(\Omega) \mid v|_{[r_i, r_{i+1}]} \in \mathbb{P}_1, i = 0, \dots, M-1\}. \quad (70)$$

A basis for this space is given by $(\phi_j)_{j=1}^{M-1}$, where:

$$\phi_j(r) = \begin{cases} \frac{r - r_{j-1}}{r_j - r_{j-1}} & \text{if } r \in [r_{j-1}, r_j], \\ \frac{r_{j+1} - r}{r_{j+1} - r_j} & \text{if } r \in [r_j, r_{j+1}], \\ 0 & \text{otherwise.} \end{cases} \quad (71)$$

We then approximate $Q(\tau, r)$ by:

$$Q_h(\tau, r) = \sum_{j=1}^{M-1} Q_j(\tau) \phi_j(r). \quad (72)$$

The variational formulation is required to hold for every test function in S_h , that is, for each ϕ_i . Substituting Q by Q_h in the weak formulation yields the following system of ordinary differential equations:

$$-\frac{d}{d\tau} \int_{\Omega} Q_h \phi_i dr + \int_{\Omega} \kappa(\gamma - r) \frac{\partial Q_h}{\partial r} \phi_i dr - \frac{1}{2} \sigma^2 \int_{\Omega} \frac{\partial Q_h}{\partial r} \frac{\partial \phi_i}{\partial r} dr - \int_{\Omega} r Q_h \phi_i dr = 0, \quad (73)$$

for all $i = 1, \dots, M-1$.

Let us denote the vector of unknown coefficients by:

$$Q_h(\tau) = [Q_1(\tau), Q_2(\tau), \dots, Q_{M-1}(\tau)]^T. \quad (74)$$

The system can then be written in matrix form as:

$$-M \frac{dQ_h}{d\tau} + B Q_h = 0, \quad (75)$$

where the mass matrix \mathbf{M} and the stiffness matrix \mathbf{B} are defined by:

$$M_{ij} = a(\phi_i, \phi_j) = \int_{\Omega} \phi_i(r) \phi_j(r) dr, \quad (76)$$

$$B_{ij} = b(\phi_j, \phi_i) = \int_{\Omega} \left[\kappa(\gamma - r) \frac{d\phi_j}{dr}(r) \phi_i(r) - \frac{1}{2} \sigma^2 \frac{d\phi_j}{dr}(r) \frac{d\phi_i}{dr}(r) - r \phi_j(r) \phi_i(r) \right] dr. \quad (77)$$

7.4 Analysis of the ODE System

To study this system of ODEs, we discretize in time using the Crank–Nicolson method. We use the same temporal mesh as before. The Crank–Nicolson scheme for this matrix ODE is given by:

$$\mathbf{M} \frac{Q_h^{n+1} - Q_h^n}{\Delta\tau} = \frac{1}{2} \mathbf{B} (Q_h^{n+1} + Q_h^n), \quad (78)$$

where $Q_h^n(\tau) = [Q_1(\tau_n), Q_2(\tau_n), \dots, Q_{M-1}(\tau_n)]^T$.

Rearranging, we obtain the linear system for $n = 0, 1, \dots, N - 1$:

$$\left(\mathbf{M} - \frac{\Delta\tau}{2} \mathbf{B} \right) Q_h^{n+1} = \left(\mathbf{M} + \frac{\Delta\tau}{2} \mathbf{B} \right) Q_h^n. \quad (79)$$

Boundary conditions are imposed using the analytical solution, and the initial condition is given by:

$$\forall r \in \Omega, \quad Q_h(\tau = 0, r) = 1. \quad (80)$$

7.5 Implementation in Python

For the implementation of this method, the same parameters are used:

$$\kappa = 0.1, \quad \gamma = 0.05, \quad \sigma = 0.01, \quad T = 1.0, \quad r_{\max} = 0.15, \quad N = 100, \quad M = 50.$$

The Python implementation, although relatively straightforward, is computationally more demanding because it requires the precise definition of the matrices \mathbf{M} and \mathbf{B} . These matrices are computed coefficient by coefficient using, for example, the `integrate.quad` function from `scipy` to evaluate the

defining integrals. As before, Figure 9 shows the 3D plot of the numerical approximation $V(r, t)$, and Figure 10 shows the error between the numerical approximation and the analytical solution.

Figure 10 indicates that the error is on the order of 10^{-7} . Although the approximation is faithful to the analytical solution, the finite element method here is less efficient than the Crank–Nicolson method discussed in Section 6.

It is likely that higher-order approximations (e.g., using \mathbb{P}_2 or \mathbb{P}_3 finite elements) could yield even more accurate results, albeit at the expense of additional computational complexity.

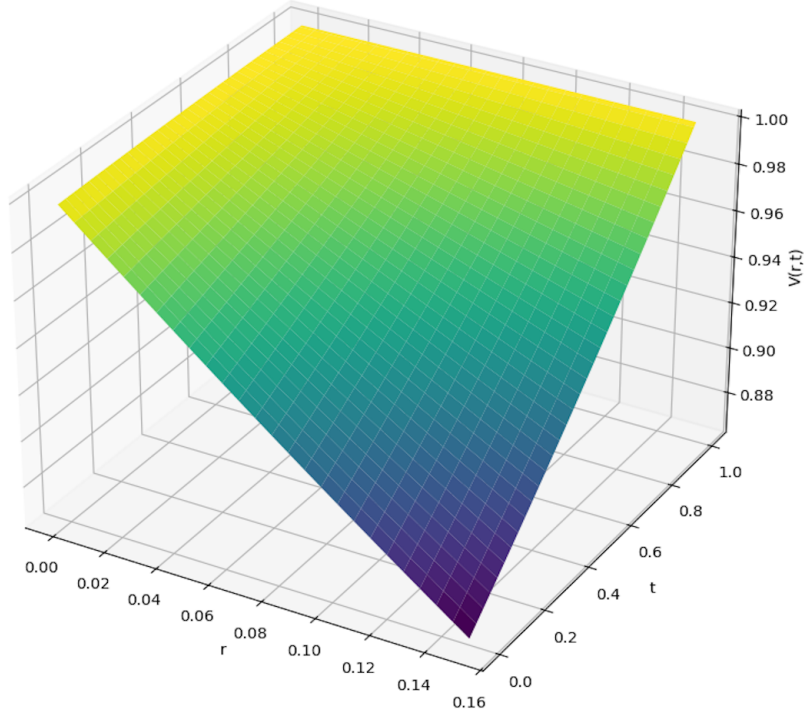


Figure 9: Approximation of the Vasicek model PDE solution using the finite element method

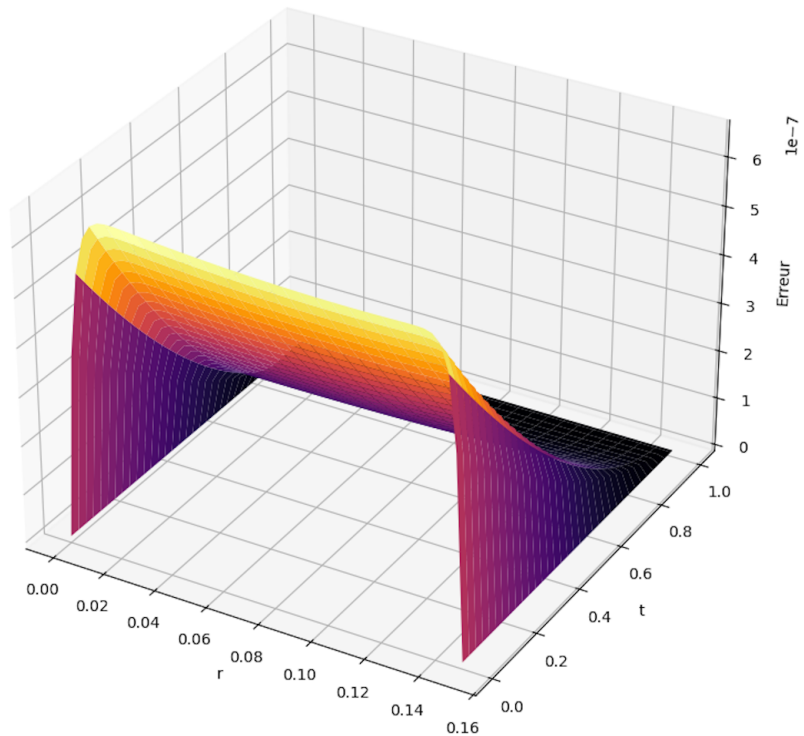


Figure 10: Error of the finite element approximation relative to the analytical solution

8 Sensitivity Analysis with Respect to Parameters

The aim of this section is to study the sensitivity of the bond price to the parameters of the Vasicek model, particularly the target rate γ and the volatility σ , which are among the most influential parameters.

In quantitative finance, the “Greeks” are used to measure the sensitivity of an option’s price to changes in a risk parameter. Although originally defined for options, the same principle applies to other financial instruments, including zero-coupon bonds. In this section, we study the partial derivatives of the bond price with respect to two key parameters of the Vasicek model: γ and σ .

Recall that under the Vasicek model, the bond price is given by

$$V(r, t) = A(t, T)e^{-B(t, T)r}, \quad (81)$$

where:

$$B(t, T) = \frac{1 - e^{-\kappa(T-t)}}{\kappa}, \quad (82)$$

$$A(t, T) = \exp \left\{ \left(\gamma - \frac{\sigma^2}{2\kappa^2} \right) \left(B(t, T) - (T-t) \right) - \frac{\sigma^2}{4\kappa} B(t, T)^2 \right\}. \quad (83)$$

8.1 Sensitivity with Respect to the Target Rate γ

The dependence on γ appears solely in $A(t, T)$. The partial derivative of V with respect to γ is given by:

$$\frac{\partial V}{\partial \gamma} = \frac{\partial A}{\partial \gamma} e^{-Br}, \quad (84)$$

with

$$\frac{\partial A}{\partial \gamma} = A \left(B - (T-t) \right). \quad (85)$$

Thus,

$$\frac{\partial V}{\partial \gamma}(r, t) = V(r, t) \left(B(t, T) - (T-t) \right). \quad (86)$$

Defining

$$f(\tau) = \frac{1 - e^{-\kappa\tau}}{\kappa} - \tau \quad \text{with} \quad \tau = T - t, \quad (87)$$

and noting that f is strictly decreasing on \mathbb{R}_+^* with $f'(0) = 0$, we obtain:

$$\frac{\partial V}{\partial \gamma}(r, t) = V(r, t)f(\tau) < 0. \quad (88)$$

An increase in the target rate γ thus reduces the present value of the bond. This result is consistent with the financial intuition that a higher target interest rate increases the discount factor (as r converges toward γ), thereby reducing the current bond price. The PDE derived from the Vasicek model is therefore coherent in its representation of the inverse relationship between bond prices and interest rates.

8.2 Sensitivity with Respect to the Volatility σ

In option pricing (particularly under the Black–Scholes model [3]), the sensitivity of the option price to the volatility of the underlying asset is of paramount importance and is denoted by the “Vega” $\nu = \frac{\partial P}{\partial \sigma}$, where P is the option price.

In our case of zero-coupon bonds, we study $\nu = \frac{\partial V}{\partial \sigma}$, where V represents the bond price. Since the dependence on σ appears only in $A(t, T)$, the partial derivative of V with respect to σ is given by:

$$\nu = \frac{\partial V}{\partial \sigma} = \frac{\partial A}{\partial \sigma} e^{-Br}. \quad (89)$$

With

$$\frac{\partial A}{\partial \sigma}(t, T) = A(t, T) \left(-\frac{\sigma}{\kappa^2} (B(t, T) - (T - t)) - \frac{\sigma}{2\kappa} B(t, T)^2 \right), \quad (90)$$

we have:

$$\frac{\partial V}{\partial \sigma}(r, t) = V(r, t) \left(-\frac{\sigma}{\kappa^2} (B(t, T) - (T - t)) - \frac{\sigma}{2\kappa} B(t, T)^2 \right). \quad (91)$$

The sign of this derivative depends on the parameters t , T , and κ .

In the Vasicek model, σ reflects the uncertainty regarding the evolution of interest rates. Since interest rate movements strongly influence bond prices, and because this influence is nonlinear, it is expected that the sign of ν varies with the other parameters.

To observe the sensitivity of the price to volatility, we simulate the distribution of zero-coupon bond prices for different values of σ at $t = 0$. Using the Euler–Maruyama scheme applied to the SDE of the Vasicek model, several trajectories of r_t are simulated for various values of σ . Then, using the simulated r_t values and the analytical solution of the Vasicek model, the bond price is computed. The histogram of the resulting bond prices is shown in Figure 11.

Recall that the Vasicek model describes the evolution of the instantaneous interest rate r_t by the Ornstein–Uhlenbeck SDE:

$$dr_t = \kappa(\gamma - r_t) dt + \sigma dW_t. \quad (92)$$

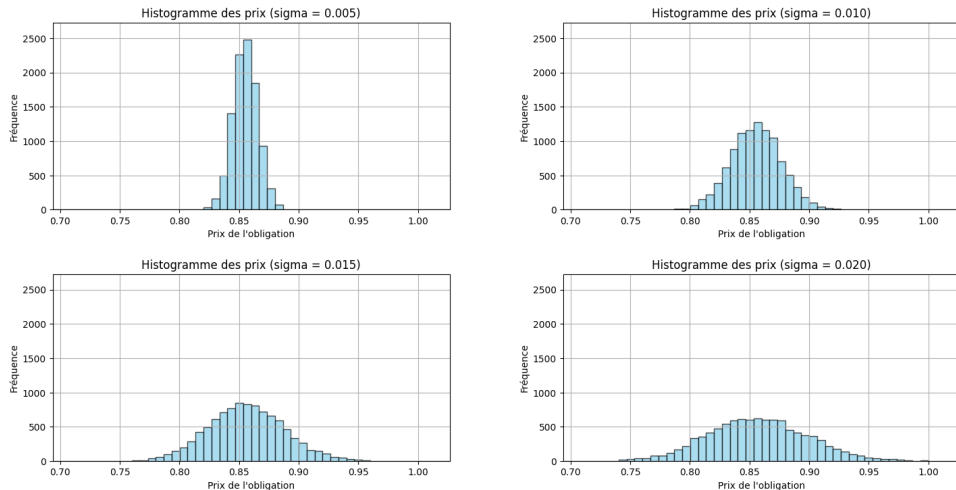


Figure 11: Simulation and comparison of zero-coupon bond price distributions at $t = 0$ for different volatilities

The parameters used are:

$$\kappa = 0.1, \quad \gamma = 0.06, \quad r_0 = 0.05, \quad \sigma = 0.01, \quad T = 3.0.$$

We observe a direct relationship between the dispersion of bond prices and volatility. When σ is low, the process r_t remains close to the target rate γ due to smaller fluctuations, leading to a more concentrated distribution of bond prices. Conversely, a higher σ results in a wider range of r_t values, leading to a greater dispersion of bond prices due to varying discount factors.

9 Conclusion

In conclusion, this work demonstrates that the pricing of zero-coupon bonds using the Vasicek model can be effectively tackled both analytically and via several numerical methods. The Euler schemes—both explicit and implicit—offer simple implementations that yield satisfactory approximations. However, the Crank–Nicolson scheme stands out for its remarkable accuracy, achieving errors on the order of 10^{-8} . The finite element approach, while providing good fidelity, does not justify the additional computational effort compared to the finite difference methods.

Finally, we have shown that the model is robust with respect to variations in the key parameters, remaining consistent and reliable—an essential property in financial mathematics where market data are often noisy or approximated.

From a numerical perspective, the use of higher-order discretization methods, such as \mathbb{P}_2 or \mathbb{P}_3 finite elements, or even finite volume methods, represents a promising avenue for further enhancing both accuracy and computational efficiency.

Moreover, by incorporating more complex boundary conditions, this work can be extended to price other financial instruments. It is also conceivable to explore more comprehensive interest rate models (e.g., Hull–White [6], CIR [5]) to test the stability of numerical schemes when additional risk factors are considered.

Bibliography

References

- [1] Oldrich Vasicek. "an equilibrium characterization of the term structure". *Journal of Financial Economics*, 5(2):177–188, 1977.
- [2] Paul A. Samuelson. Proof that properly discounted present values of assets vibrate randomly. *The Bell Journal of Economics*, 4(2):369–374, 1973.
- [3] Fischer Black and Myron Scholes. The pricing of options and corporate liabilities. *Journal of Political Economy*, 81(3):637–654, 1973.
- [4] Robert C. Merton. On the pricing of corporate debt: The risk structure of interest rates. *The Journal of Finance*, 29(2):449–470, 1974.
- [5] John C. Cox, Jonathan E. Ingersoll, and Stephen A. Ross. A theory of the term structure of interest rates. *Econometrica*, 53(2):385–407, 1985.
- [6] John Hull and Alan White. Pricing interest-rate-derivative securities. *The Review of Financial Studies*, 3(4):573–592, 1990.
- [7] Wikipedia contributors. Tridiagonal matrix algorithm. Wikipedia, The Free Encyclopedia. Page consultée le 12 février 2025.
- [8] Paolo Baldi. *Stochastic Calculus: An Introduction through Theory and Exercises*. Universitext. Springer, 2017.